CERAMIC/METAL NANOCOMPOSITES: LYOPHILIZATION AND SPARK PLASMA SINTERING

C.F. Gutierrez-Gonzalez[1], S. Agouram[2], R. Torrecillas[1], J.S. Moya[3] and S. Lopez-Esteban[3]*

[1]Centro de Investigación en Nanomateriales y Nanotecnología (CINN) [Consejo Superior de Investigaciones Científicas (CSIC)-Universidad de Oviedo (UO)-Principado de Asturias (PA)]; Parque Tecnológico de Asturias, 33428 Llanera (Spain).
[2]Dept. of Applied Physics and Electromagnetism, Univ. Valencia, 46100 Burjassot (Spain).
[3]Instituto de Ciencia de Materiales de Madrid (ICMM), Consejo Superior de Investigaciones Cientificas (CSIC), Cantoblanco, 28049 Madrid (Spain).

* Corresponding author (s.lopez.esteban@csic.es)

Keywords: *Lyophilization, Freeze-drying, Composites, Nanostructure, Epitaxial growth, Transmission Electron Microscopy, Spark Plasma Sintering.*

1 General Introduction

Due to their interesting properties and applications, nanostructured materials are nowadays the object of one of the most outstanding lines of research. Concerning ceramics, it is well known that the presence of a nanometric microstructure is responsible for the enhancement of different properties, such as mechanical [1,2], catalytic [3,4] optical [5,6]. Numerous techniques have been developed to produce nanoparticles, among which the ones that are increasing in popularity are vapour-phase synthesis (CVD [7,8], spray pyrolysis [9,10], laser pyrolysis [11,12]) or wet routes such as sol–gel [13,14].

This work is focused on ceramic-based nanocomposites formed by oxide ceramic matrices with well-dispersed metal and/or semiconductor nanoparticles are promising materials for structural and multifunctional applications [15]. A broad spectrum of synthesis techniques has been used with different ceramic/metal systems. Unfortunately, the use of nanosized powders involves dealing with the strong tendency of the nanoparticles to agglomerate. In order to avoid this negative effect, using wet processing routes of colloidal suspensions followed by a fast drying method has become one of the most active research areas in ceramics. In this context, the interest of this work is to synthesize highly homogeneous, pure and reproducible ceramic/metal nanocomposites with an average metal particle size in the nanometric range, obtained from powders spray-freezed and lyophilized. The cryochemical route proposed, followed by Spark Plasma Sintering (SPS) of the powders leads to compacts with excellent mechanical features.

2 Experimental Methods

2.1. Starting materials

The following commercially available powders have been used as raw materials: (1) tetragonal zirconia polycrystals (3Y-TZP, 3 mol% Y2O3; TZ-3YE, Tosoh Corp.), with an average particle size of d50 = 0.26±0.05 microns and (2) nickel (II) nitrate hexahydrate (Merck, Germany, 99.0% purity, $Ni(NO_3)_2 \cdot 6H_2O$).

2.2. Synthesis

Nickel nitrate salt powders were dispersed in distilled water by ultrasonic agitation in a suitable volume to achieve total dissolution. The ceramic powder was added in order to obtain zirconia/Ni composites with a metal content of 1 vol% Ni, 2.5 vol% Ni and 3.5 vol% Ni. The corresponding samples have been denoted as LF1, LF2.5 and LF3.5, respectively.

The suspensions were milled for 24 hours with zirconia balls in order to get an homogeneous slurry. As the materials were prepared in distilled water in order to be subsequently lyophilized, the stability of the dispersions was specifically studied in aqueous media. Several suspensions with different wt.% solid content were prepared with different additions of an alkali-free organic polyelectrolyte as surfactant for different relative proportions of metal. The sedimentation behaviour of the water-based slurries was studied at room temperature in glass test tubes for times up to 24 h. Finally, the best homogeneity was reached by the suspensions with 70 wt.% solids and 1 wt.% surfactant. TEM studies made on selected samples corroborate these results.

The mixture was sprayed over liquid nitrogen with an airbrush gun (Iwata Custom Micron SB airbrush, Iwata Medea, Inc., Portland, OR, USA) equipped with a 0.18 mm diameter nozzle. The frozen suspension was subsequently freeze-dried for 48 h in a lyophilizer (Cryodos-50, IMA-TELSTAR, S.L., Barcelona, Spain) until completely dried. The temperature of the cold finger in this equipment is continuously set at -50± 2ºC. The freeze dryer shelf temperature and the chamber pressure during the entire process were +20±2ºC and 0.06±0.01 mbar, respectively. These conditions, according to the Phase Diagram of water, correspond to water vapor.

The resulting powder was calcined at 600ºC for 2 hours in air to obtain ZrO_2/NiO powders [16]. Finally, the metal oxide was reduced to metallic nickel in a 90%Ar/10%H_2 atmosphere at 500ºC for 2 h, obtaining a zirconia powder with metal nanoparticles adhered to the surface of the ceramic grains (zirconia/nNi).

Subsequently, the different powders were spark plasma sintered (SPS, FCT Systeme GMBH, HPD 25, Germany) under the conditions 1350ºC, 25 kN, 5 min in hydrogen atmosphere.

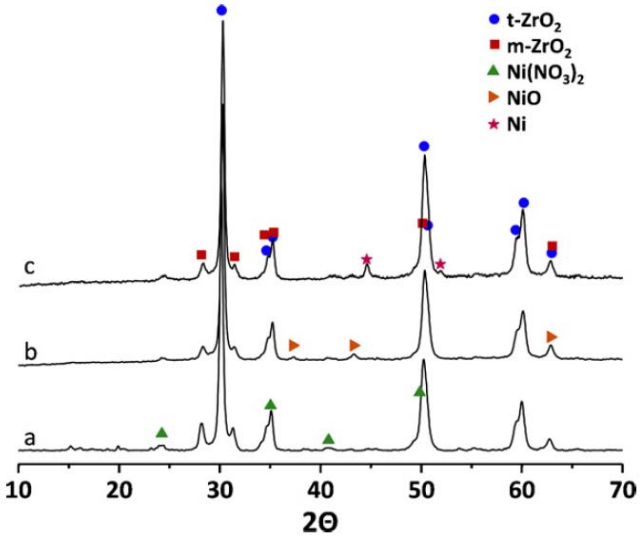

Figure 1. X-ray diffractograms corresponding to the nanopowder with LF3.5 obtained at different stages of the processing route: (a) lyophilized 3Y-TZP/Ni$(NO_3)_2$ 6H_2O, (b) calcined 3Y-TZP/NiO, and (c) reduced 3Y-TZP/Ni.

2.3. Characterization

X-ray diffraction analysis of the nanopowders at different stages of the processing route was used for phase identification using Cu Ka radiation (XRD Bruker AXS D8 ADVANCE, with a SolX energy-dispersive detector).

Further characterization of the samples was performed by transmission electron microscopy (TEM), high resolution TEM (HRTEM) and energy dispersive X-ray spectroscopy (EDX-mapping) by using a field emission gun (FEG) TECNAI G2 F20 microscope operated at 200 kV. In order to prepare the TEM samples, the ZrO_2/Ni powder specimens were treated by sonicating in absolute ethanol for several minutes, and a few drops of the resulting suspension were deposited onto a holey-carbon film supported on a copper grid, which was subsequently dried. The samples were also used to determine the elemental content by EDX.

The hardness was measured on 30 samples for each group (in terms of composition and drying

method) in a Vickers diamond microindenter (Leco 100-A Microindentation Hardness Testing System, USA) on surfaces of cross sections polished down to 1 micron, with an applied load of 0.9 kg (8.8 N) for 15 s. The hardness was determined according to the equation HV = 1.853P/d2, where P stands for the applied load (in N) and d stands for the diagonal length of the indentation (in mm). Pure zirconia was studied as control.

3 Results and Discussion

3.1. X-ray diffraction

Figure 1 shows the X-ray diffractograms of sample LF3.5 in the range 10º–70º obtained at different stages of the processing route. The results confirm that products at the first stage consisted only of zirconia and nickel nitrate with no presence of any other phases (Figure 1a). After calcination, the nickel nitrate was oxidized into NiO (Figure 1b). No presence of either nickel nitrate or nickel oxide was detected in the final powder, which consisted only of zirconia/nNi (Figure 1c). The same results were obtained for the other two compositions (LF1 and LF2.5).

3.2. Transmission electron microscopy (TEM)

A representative TEM-EDX spectrum is shown in Figure 2. In the spectrum, it is possible to discern clearly the presence of Zr, O and Ni peaks. The C and Cu peaks are due to the TEM holey carbon-Cu grid.

Figure 3 shows a typical HRTEM micrograph of size and distribution of Ni nanoparticles. The metal particles obtained are in the nanometer range and appear homogeneously and well dispersed on the zirconia surface.

More than 100 particles from all over the sample were measured to determine the Ni particle size distribution for each composition. As shown in Figure 3, the mean size of the nickel nanoparticles increases with the Ni content. In the sample with 1 vol% Ni the particle size distribution is narrow and centred around 16–19 nm. Samples prepared with 2.5 and 3.5 vol% Ni present a broader distribution, between 20–30 nm and 22–42 nm. In all cases, the nanoparticles average size is lower than 35 nm.

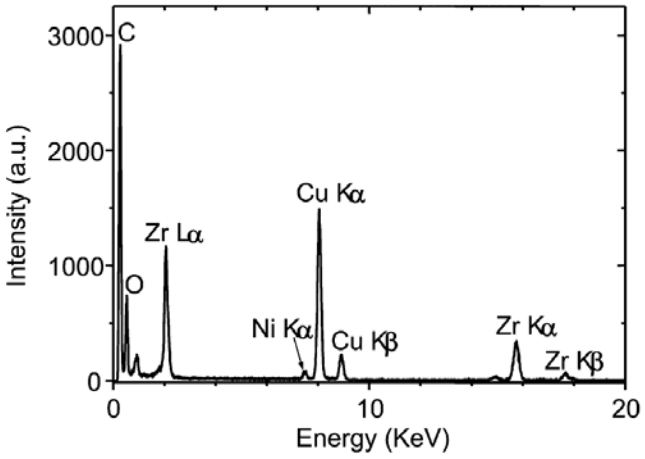

Figure 2. TEM-EDX spectrum of LF3.5 sample.

The results of the method described have been compared with those of samples dried in furnace. For both methods, the mechanical performance of the materials is excellent.

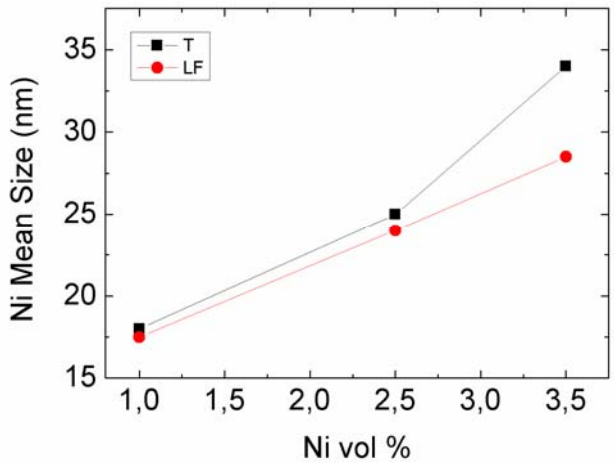

Figure 3. Nickel nanoparticles mean size in ZrO_2/Ni powders obtained by lyophilization (LF) and by drying in furnace (T).

3.3. HRTEM characterization

3.3.1. Ceramic submicron particles

A closer view of the nanostructure of the ZrO_2 matrix after deposition of the Ni nanoparticles with different content of Ni was carried out by HRTEM (Figure 4). It has been observed the clear lattice spacing indicating that the nanoparticles are highly crystallized with an interplanar spacing of 2.62 A˚, corresponding to the (002) planes of ZrO_2; the spacing of 2.55 A˚ between adjacent lattice planes corresponds to the (110) planes of ZrO_2; another interplanar distance of 1.82 A˚ corresponds to (112) planes of ZrO_2.

Fast Fourier Transform (FFT) pattern of selected zones clearly illustrates the monocrystalline structure which could be indexed by a tetragonal phase, space group P42/nmc (137) in [–110] zone axis ZA (JCPDS: 83–113). Similar features were observed for other samples with different contents of Ni.

3.3.2. Nickel nanoparticles

Figure 5A presents a high resolution TEM micrograph of the 3Y-TZP/Ni powder with 2.5 vol% Ni, showing the Ni nanoparticles identified by EDX mapping. High resolution TEM image and the FFT pattern of the selected zone are presented in Figure 5B and Figure 5C. The Ni nanoparticles appear as discrete, uniform and crystalline with a size around 20 nm. The Ni nanoparticles show a well defined lattice spacing of 2.05 A˚, corresponding to the (111) planes of face-centred cubic phase of Ni, space group Fm3m (225) (JCPDS: 4-850).

In all cases, these powders present an accurate composition, homogeneity and a good dispersion of metal. Likewise, the Ni nanoparticles are firmly attached to the zirconia particles, avoiding their coalescence, with an interface ordered, very neat, showing that the Ni nanoparticles have grown epitaxially on the surface of zirconia.

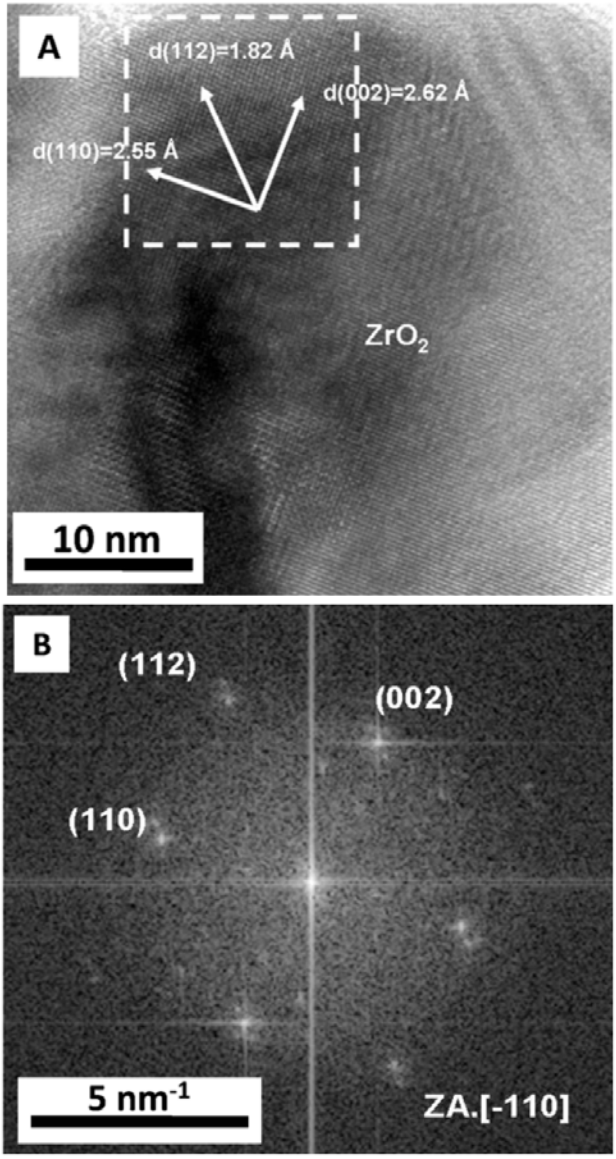

Figure 4. (A) HRTEM micrograph corresponding to LF2.5. (B) Fast Fourier Transform pattern of the selected area.

3.3.3. Ceramic/metal interface

Further structural characterization of the powders was carried out using HRTEM to study the nature of the interface between the Ni nanoparticles and the zirconia matrix. Figure 6 illustrates a representative micrograph. The interface is ordered, very neat, showing that the Ni nanoparticles have grown epitaxially on the surface of zirconia. This effect has already been observed in samples obtained by a different drying method [17].

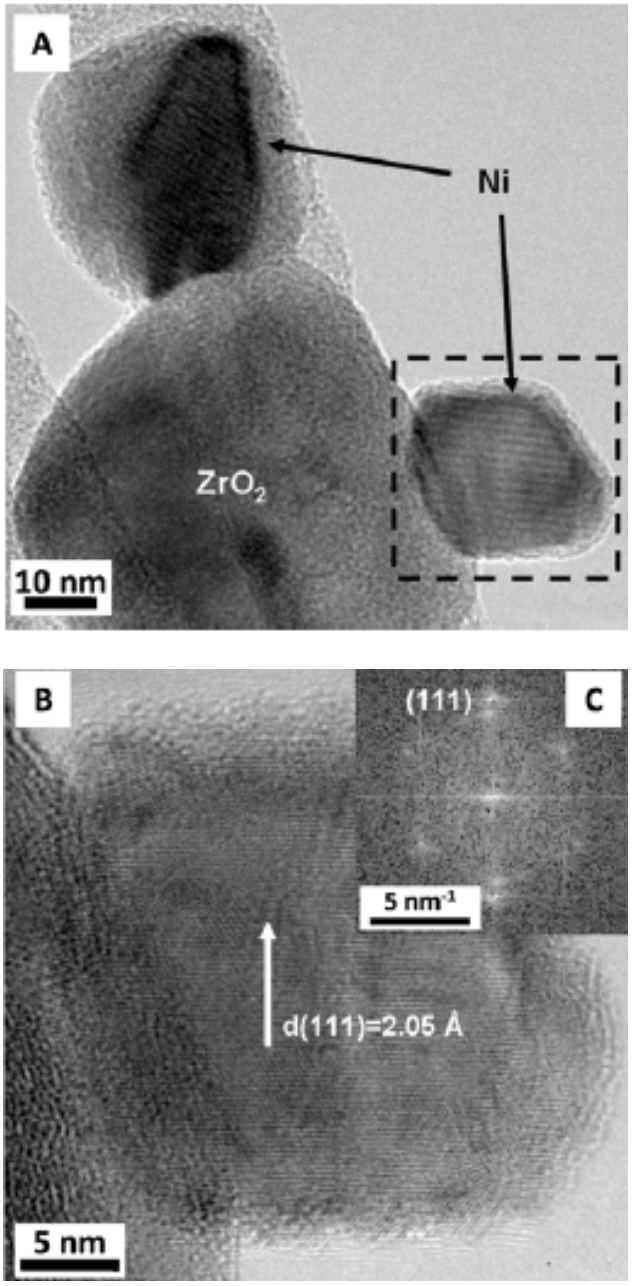

Figure 5. (A) HRTEM micrograph of the 3Y-TZP/Ni powder with 2.5 vol% Ni showing the Ni nanoparticles identified by EDX mapping. (B) Detail of Ni nanoparticle and the corresponding index assignment. (C) FFT pattern of a Ni nanoparticle.

The origin of such a good degree of epitaxy in 3Y-TZP/Ni nanocomposites can be due to two reasons: (i) a very good lattice matching between ZrO_2 and nickel and (ii) the ‘‘evaporation–condensation’’ grain growth mechanism present in metallic nanoparticles. The combined effect of these factors produces a real epitaxial growth of Ni crystals on ZrO_2 submicron grains. This feature is positive as, theoretically, it may lead to excellent mechanical properties in the corresponding sintered materials. Therefore, the future work will be focused on investigating different sintering routes and, subsequently, the features of the dense materials [18].

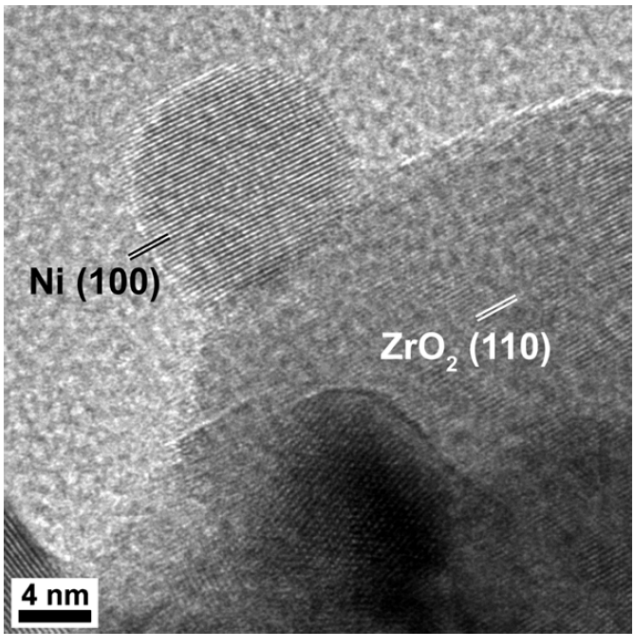

Figure 6. HRTEM micrograph of Ni nanoparticle epitaxially grown on the surface of zirconia submicron particle. The interface between both particles presents an excellent matching of atomic planes.

3.4. Mechanical characterization

As expected by taking into account other works [16], the presence of Ni nanoparticles increases the hardness respect to the value of pure zirconia. For both methods, the mechanical performance of the materials is excellent. The highest increase is 30% with respect to the hardness of pure zirconia, and corresponds to the composites with a metal content of 1 vol.% Nickel (Figure 7). There is no contradiction of these results with those presented elsewhere, where the maximum was found for samples

with 2,5 vol. % Ni, because in the present study the range of composition is much more narrow and, therefore, easier to reach a more accurate result. The hardness of the sintered materials is similar for both methods, as the size of the Ni nanoparticles was similar in the original composite powders.

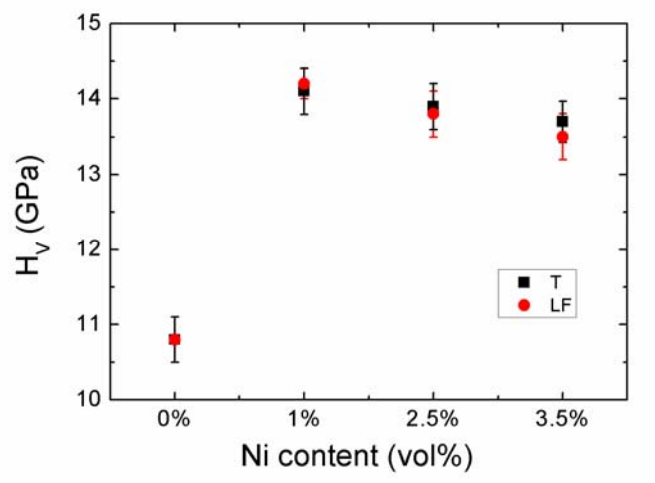

Figure 7. Vickers hardness of ZrO_2/Ni nanocomposites obtained by lyophilization (LF) and by drying in furnace (T) for increasing volume contents of Ni. The value corresponding to pure zirconia has been plotted for comparison purposes.

4 Conclusions

This work demonstrates that combining spray-freezing with lyophilization is a feasible technique for preparing high-quality ceramic/metal nanostructured powders that lead to compacts with excellent nanostructures and mechanical features.

References

[1] S. Hao, H. Wang, Adv. Mater. Res. 168-170 (2011) 1846-1849.

[2] M. Yi, C. Xu, J. Zhang, Z. Jiang, Adv. Eng. Mater. 154-155 (2011) 1356-1360.

[3] A. Folli, I. Pochard, A. Nonat, U.H. Jakobsen, A.M. Shepherd, D.E. Macphee, J. Am. Ceram. Soc. 93 (2010) 3360-3369.

[4] D. Thiele, Mater. Chem. and Phys. 124 (2010) 529-534.

[5] R.M. Krsmanović, Z. Antić, M.G. Nikolić, M. Mitrić, M.D. Dramićanin, Ceram. Int. 37 (2011) 525-531.

[6] Y. Zorenko, T. Voznyak, V. Gorbenko, E. Zych, S. Nizankovski, A. Dan'Ko, V. Puzikov, J. Lumin. 131 (2011) 17-21.

[7] J.H. Kim, S.K. Lee, O.M. Kwon, D.S. Lim, J. Nanosci. Nanotechno. 9 (2009) 4121-4127.

[8] K. Kubota, Int. J. Jpn. Soc. Precis. Eng. 76 (2010) 1336-1339.

[9] H.Y. Koo, J.H. Kim, Y.N. Ko, Y.C. Kang, V.D. Nguyen, D. Byun, B.K. Kim, J. Ceram. Soc. Jpn. 118 (2010) 613-616.

[10] M.I. Martín, L.S. Gómez, O. Milosevic, M.E. Rabanal, Ceram. Int. 36 (2010) 767-772.

[11] R. Dez, F. Ténégal, C. Reynaud, M. Mayne, X. Armand, N. Herlin-Boime, J. Eur. Ceram. Soc. 22 (2002) 2969-2979.

[12] A. Müller, N. Herlin-Boime, F. Ténégal, X. Armand, F. Berger, A.M. Flank, R. Dez, K. Müller, J. Bill, F. Aldinger, J. Eur. Ceram. Soc. 23 (2003) 37-46.

[13] M. Miranda, A. Fernández, E. Saiz, A.P. Tomsia, R. Torrecillas, Int. J. Mater. Res. 101 (2010) 117-121.

[14] R. Torrecillas, M. Díaz, F. Barba, M. Miranda, F. Guitián, J.S. Moya, J. Nanomater. (2009) art nº 498505.

[15] J.S. Moya, S. Lopez-Esteban and C. Pecharroman, "*The challenge of ceramic/metal*

microcomposites and nanocomposites". Progress in Materials Science (2007) 52:1017-1090.

[16] F. Esteban-Betegon, S. Lopez-Esteban, J. Requena, C. Pecharroman, J.S. Moya, J.C. Conesa, "*Obtaining Ni Nanoparticles on 3Y-TZP Powder from Nickel Salts*". Journal of the American Ceramic Society (2006) 89:144-150.

[17] C. Pecharroman, J.I. Beltran, F. Esteban-Betegon, S. Lopez-Esteban, J.F. Bartolome, M.C. Munoz, J.S. Moya, "*Zirconia/nickel interfaces in micro- and nanocomposites*", Z. Metallkd. 96 (2005) 507–514.

[18] C.F. Gutierrez-Gonzalez, S. Agouram, R. Torrecillas, J.S. Moya, S. Lopez-Esteban, "*Ceramic/metal nanocomposites by lyophilization: Processing and HRTEM study*". Materials Research Bulletin 47 (2012) 285–289